

Formulation and *in vitro* characterization of inhalable dasatinib-nanoemulsion as a treatment potential against A549 and Calu-3 lung cancer cells

Alaa S. Tulbah* 

Department of Pharmaceutical Sciences, College of Pharmacy, Umm Al Qura University, Makkah, Saudi Arabia

Address for correspondence:

Alaa S. Tulbah,
Department of Pharmaceutical Sciences, College of Pharmacy, Umm Al Qura University, Makkah, Saudi Arabia.
E-mail: astulbah@uqu.edu.sa

WEBSITE: ijhs.org.sa

ISSN: 1658-3639

PUBLISHER: Qassim University

Introduction

Lung cancer is a malignant tumor of the lungs caused by the unchecked growth of cells, most often those of the epithelium.^[1,2] It is responsible for one million deaths annually, making it the most lethal tumor in the world.^[1,3,4] While tobacco use is responsible for the vast majority (80–90%) of lung cancer diagnoses, many other factors have been found to be tenuously linked to the disease's development.^[1–3] Despite the fact that the various stages and subtypes of lung cancer necessitate distinct treatment modalities, surgery, chemotherapy, and radiation therapy continue to be the therapies of choice. Multiple studies have demonstrated that blocking the tyrosine kinase domain of the epidermal growth factor (EGF) receptor is an effective treatment for lung cancer.^[5–8] This is because doing so prevents the activation of signal transducers and activators of transcription pathways crucial to lung cancer.^[5–8] Dasatinib (DTB) is a multi-target drug of the second generation of tyrosine kinase inhibitors that have been used for the treatment of lung, prostate, and ovarian malignancies, in addition to chronic

ABSTRACT

Objective: Dasatinib (DTB) is a second-generation tyrosine kinase inhibitor that was found it could help with lung cancer treatment. However, DTB has low aqueous solubility and poor bioavailability due to its incomplete absorption and high first-pass effect. The objective of this study was to improve DTB's solubility, delivery, and efficacy as a potential lung cancer treatment by developing an inhalable DTB-nanoemulsion (DNE) formulation.

Methods: The DNE formulation was prepared by the spontaneous emulsification method, using oleic acid as the oil phase and a mixture of Kolliphor RH 40 and dipropylene glycol as surfactant. Compared with free DTB, the DNE formulation enhanced the aqueous solubility, flow property, and delivery of DTB to the lungs with a good fine-particle dose, fine-particle fraction, and mass median aerodynamic diameter.

Results: The DNE formulation was safe on lung cancer cells when the cell viability and toxicity were evaluated and IC₅₀ values were found to be 0.0431 µg/mL and 0.0443 µg/mL on A549 and Calu-3 cells, respectively. Moreover, DNE formulation significantly increased its anti-cancer effectiveness against A549 and Calu-3 lung cancer cells by interfering with cell cycle progression through apoptosis or cell cycle arrest.

Conclusion: The nanoemulsion formulation has the potential to be an effective carrier for DTB, which could possibly be used to treat lung cancer.

Keywords: Aerodynamic, apoptosis, cytotoxicity, dasatinib, lung cancer

myeloid leukemia.^[8–10] DTB blocks the tyrosine kinase domain of the EGF receptor, which, as explained above, prevents activation of signal transducers and activators of transcription pathways crucial to lung cancer.^[5–8] However, DTB is a biopharmaceutical class II medication with very weak and pH-dependent solubility.^[10,11] Due to its inadequate absorption and high first-pass impact, DTB has poor bioavailability.^[10,11] If this can be overcome, improved treatment efficacy and reduced systemic toxicity may result from the development of safe and efficient DTB delivery vehicles.

A major roadblock in the creation of new pharmaceutical formulations is, therefore, the improvement of DTB medicines' solubility in water to enhance their oral bioavailability.^[12,13] Numerous studies have been undertaken to enhance DTB's medication release and oral bioavailability.^[14–16] To achieve rapid results against leukemia, Mohan and Sangeetha successfully developed an immediate-release tablet form of DTB.^[14] To improve DTB's solubility, Parvataneni *et al.* produced spherical micelles of the compound enclosed by

lactose monohydrate and sodium lauryl sulfonate.^[15] DTB lipid nanoparticles were developed by Begum and Gudipati to improve their solubility.^[16] However, assessments of the available literature indicate that no research has been conducted into the creation of an inhalable delivery method of a DTB nanoemulsion formulation. Nanoemulsions are nano-sized emulsions that are thermodynamically stable and consist of two immiscible liquids (water and oil).^[15,16] Nanoemulsion formulations have many benefits, including a high solubilization capacity for both hydrophobic and hydrophilic drugs, enhanced lymphatic absorption, and reduced reliance on first-pass metabolism.^[17,18] As an alternative to the more traditional routes of administration, pulmonary drug delivery has become an integral part of the pharmaceutical industry.^[19-22] Nebulizer inhalation therapy is advantageous because it allows for the simultaneous administration of many drugs, is simple to use with tidal breathing, safe for use with all age groups, can be modified for use with extremely ill patients, and produces a visible spray.^[20,22,23]

This research aimed to create an inhalable nanoemulsion formulation of DTB to enhance its delivery, solubility, bioavailability, and efficacy as a potential treatment for lung cancer. An inhalable DTB nanoemulsion formulation has the potential to increase the drug's bioavailability, efficacy, and safety by enhancing its aqueous solubility. The physicochemical properties and *in vitro* aerosol deposition of the DTB nanoemulsion formulation were analyzed. The cytotoxicity (effects on cell proliferation, apoptosis, and cell cycle progression) of the formulation was also evaluated *in vitro* using human lung adenocarcinoma cell lines A549 and Calu-3.

Materials and Methods

Materials

DTB was obtained from Xian Lukee Bio-Tech Co., Ltd., located in XI'AN, China. Dipropylene glycol, Kolliphor RH 40, glycerol, and oleic acid were procured from Sigma-Aldrich, Germany. Acetonitrile, methanol, glacial acetic acid (analytical grade), and trifluoroacetic acid were all purchased from Thermo-Fisher, Europe. Lung cancer cell lines A-549 and Calu-3 were purchased from Nawah Scientific Inc. (Mokatam, Cairo, Egypt).

Preparation of DTB-nanoemulsion (DNE)

The spontaneous emulsification method was employed to prepare the DNE formulation.^[24] Briefly, DTB (10 mg) was dissolved in oleic acid and Kolliphor RH 40 and dipropylene glycol was added to the mixture at 20°C to form the mixed oil phase. Glycerol was added to water to form the aqueous phase. Then, the oil phase was gradually mixed with the aqueous phase using an overhead stirrer (IKA@ RW 20 Digital, Nara, Japan) for 30 min at a speed of 300 rpm. After that, the emulsion was homogenized in a high-shear homogenizer at 10,000 rpm for 15–20 min.

In vitro evaluation of DNE

High-performance liquid chromatography (HPLC)

Quantification of DTB

The HPLC technique was used to determine the concentration of DTB with a Kromasil column (4.6 × 150 mm, 5 μm) as described by Alarjah *et al.*^[25] The mobile phase was an aqueous solution of 0.2% acetic acid and 0.1% trifluoroacetic acid, with the pH adjusted to 3.5 and acetonitrile (65:35) using a gradient elution at a flow rate of 1 mL/min, with 100 μL, an injection volume, and a wavelength of 314 nm used for DTB detection.

Equilibrium solubility studies

After adding 10 mL of oil phase to a predetermined amount of DTB, the mixture was agitated in a thermostatically controlled shaker at 37 ± 0.5°C for 72 h. For 10 min, the oily phase was centrifuged at 12,000 rpm. Using the previously described HPLC in triplicate, the drug content of the supernatant was determined.

Measurement of drug content and encapsulation efficiency (EE)

To determine the drug content, 500 μL of DTB nano-emulsion sample was diluted with acetonitrile (1:1) and then diluted again after sonication with water: Acetonitrile (1:1). Using the previously described HPLC in triplicate, the drug content of the resulting solution was determined.^[26]

The EE of the produced nanoemulsion was determined by centrifugation.^[21] 500 μL of DTB nano-emulsion sample was added to a nanosep, then centrifuged at 7000 rpm for 30 min to separate the unencapsulated drug. The suspension above the nanosep filter was completed to 500 μL with water and diluted with acetonitrile (1:1) and then diluted again after sonication with water: acetonitrile (1:1). Using the previously described HPLC in triplicate, the drug concentration of the resulting solution was calculated.

Measurement of morphology

The morphology and size of the DNE formulation were quantified using transmission (Plus) electron microscopy (JEM-2100, JEOL, Japan).^[19] One drop of nanoemulsion was placed on a carbon-coated transmission electron microscopy (TEM) grid with a mesh size of 200 and allowed to dry. The grid was stained with phosphotungstic acid, and TEM pictures were captured at 120 kV at varying magnifications.

Analysis of thermal properties

To determine the temperature state, compatibility, and crystallinity of the components of the DNE formulation, differential scanning calorimetric (DSC-60A, Shimadzu, Japan) was used.^[27] Samples of DNE, DTB, and plain nanoemulsion formulation were sealed in an aluminum pan and subjected to a heating scan from 25 to 300°C at a rate of 10°C/min (under nitrogen gas) and with a flow rate of 10 mL/min.

Aerodynamic characterization

The British Pharmacopoeia (2005) included Appendix XII F, which outlined the fundamental procedure for aerodynamic characterization.^[28] To ascertain the aerodynamic properties of the DNE formulation, the Andersen MKII Cascade Impactor (ACI) was used. All ACI components were cleaned in the mobile phase, and silicone fluid was sprayed onto the plates. All ACI components were sealed with parafilm M laboratory film after assembly. At a flow rate of 15 L/min, each DNE sample (12.338 µg) was nebulized (jet nebulizer) and introduced into the ACI device^[29,30] Five independent measurements ($n = 5$) were performed using a validated HPLC method to determine the amount of medication deposited at each stage after rinsing with the mobile phase. Impactor data analysis software (CITDAS, Copley Scientific, UK) evaluated the total emitted dose (TED), fine-particle dose (FPD, g), fine-particle fraction (FPF%), and mass median aerodynamic diameter (MMAD, m).

In vitro cytotoxicity of DNE

Lung cancer cell lines A549 (5×10^3 cells/well) and Calu-3 were maintained in DMEM media with 100 mg/mL of penicillin/streptomycin, and 10% of heat-inactivated fetal bovine serum. Until confluency was attained, cells were grown in a humidified incubator with 5% CO₂ at 37°C.^[31]

Cell viability and cytotoxicity were evaluated using the sulphorhodamine B (SRB) assay in A549 and Calu-3 lung cancer cell lines.^[32] Briefly, 96-well plates were seeded with 100 µL from a cell suspension of 5×10^3 cells. The plates were incubated for 24 h and then treated with DNE formulation (0.001–100 µg/mL) and free DTB suspension (0.001–100 µg/mL). Following 72 h of exposure, the cells were fixed with trichloroacetic acid and incubated at 4°C for 1 h. Following this, the cells were rinsed with water and incubated in 70 L, 0.4% w/v-SRB solution for 10 min at 25°C in the dark. The plates were washed 3 times with 1% acetic acid and dried overnight in the air. A protein-bound SRB stain was used to dissolve it in TRIS (150 µL, 10 mM). Absorbance was measured at 540 nm using an Omega microplate reader (BMG LABTECH®-FLUOstar, Ortenberg, Germany). Cell viability was determined, as previously stated, by comparing the percentage of live cells to those in the untreated control.^[33] The drug's IC₅₀ concentration was determined as the concentration at which cell viability dropped by 50%. The IC₅₀ values were determined by constructing a plot of the proportion of living cells to the concentration (µg/mL).

Cell cycle assay

The effect of the DNE formulation was assessed on the cell cycle phases of A549 and Calu-3 lung cancer cell lines after 24 h and 48 h using flow cytometry assay.^[34] After 24 and 48 h of treatment, 10⁵ cells were harvested through trypsinization and washed twice with ice-cold phosphate-buffered saline (PBS, pH 7.4) and 60% ice-cold ethanol and then fixed by incubating them at 4°C for 1 h. After being fixed, the cells were washed twice with PBS and then suspended in 1 mL of PBS with 50 g/mL RNAase A and 10 µg/mL propidium iodide (PI)

for 20 min in the dark at 37°C. Flow cytometry analysis was performed with anFL2 ($\lambda_{ex/em}$ 535/617 nm) signal detector (ACEA Novocyte™ flow cytometer, ACEA Biosciences Inc., San Diego, CA, USA) to determine the cell cycle distribution.

Apoptosis assay

The impact of the DNE formulation on the proportions of cells undergoing programmed cell death, apoptosis, and necrosis was determined using the apoptosis detection kit (Abcam Inc., Cambridge Science Park, Cambridge, UK) in conjunction with two-fluorescent-channel flow cytometry.^[35-37] After 24 and 48 h of treatment, 10⁵ cells were harvested through trypsinization and washed twice with ice-cold (PBS, pH 7.4) and the cells were incubated in the dark with 0.5 mL of Annexin V-FITC/PI solution for 30 min. After staining, the cells were analyzed for PI fluorescent and FITC signals using FL1 and FL2 signal detectors ($\lambda_{ex/em}$ 535/617 nm for PI and $\lambda_{ex/em}$ 488/530 nm for FITC) in an ACEA Novocyte™ flow cytometer (ACEA Biosciences Inc., San Diego, CA, USA). Quadrant analysis was used to determine the total number of FITC and PI-positive cells using ACEA NovoExpress™ software (ACEA Biosciences Inc., San Diego, CA, USA).

Statistical analysis

IBM's Statistical Package for the Social Sciences 22 (USA, P 0.05) was used to conduct unpaired two-tailed t-tests and one-way analysis of variance. The results are shown as mean \pm standard deviation, with each test carried out in triplicate. A Student t-test was used in data analysis.

Results

Preparation of DNE

Preformulation studies were carried out to identify the composition of the nanoemulsion. Oleic acid was used as the oil phase due to its high solvency. The solubility of DTB in oleic acid was measured and found to be 25.86 ± 3.04 mg/mL.

In addition, Kolliphor RH 40 was used as a nonionic solubilizer and emulsifying agent due to its ability to produce a stable small-sized nanoemulsion with a high percentage EE for a long time.^[35,36] To produce a nanoemulsion with small droplet size and narrow size distribution, a lower temperature was helpful. To prepare the nanoemulsion, a temperature of 20°C was chosen that demonstrated a strong connection at the oil-water interface using RH 40. Dipropylene glycol was used as a cosurfactant and because the nanoemulsion's drug-loading capacity and droplet size were thoroughly taken into account, a formulation composed of oleic acid (4.5 mL) with a mixture (3 mL) of Kolliphor RH40 and dipropylene glycol was selected to prepare the DNE. The DNE formulation was successfully prepared by the spontaneous emulsification method as shown in Table 1, using oleic acid as the oil phase and Kolliphor RH40/dipropylene glycol as surfactant.

Table 1: Composition and *in vitro* characterization of DTB-nanoemulsion formulation

Formulation code	Oleic acid (mL)	Kolliphor RH40 (mL)	Dipropylene glycol (mL)	Glycerol (mL)	Water	EE (%) (Mean±SD)	Drug content (µg/mL) (Mean±SD)	Particle size (nm) (Mean±SD)	PDI (Mean±SD)
DTB-nanoemulsion	4.5	2.5	0.5	1.5	Up to 100 mL	96.74±1.595	9.46±0.139	40.72±4.037	0.26±0.02

SD: Standard deviation

In vitro evaluation of DNE

HPLC quantification of DTB

The method developed by Alarjah *et al.* was used to quantify the content of DTB.^[25] The DTB peak was measured at 5.448 min of retention time. Between 0.195 and 6.25 µg/mL, linearity was achieved with a coefficient of determination (R^2) of 0.999.

Measurement of drug content and EE

The results of Table 1 show that the aqueous solubility of DTB was successfully increased by using the nanoemulsion formulation and this was confirmed by the results of drug content measurement. Compared with the aqueous solubility of DTB (14.95 ± 2.56 µg/mL), the solubility of DTB in the nanoemulsion was significantly ($P < 0.05$) increased, thus enhancing its anti-cancer and bioavailability effectiveness. DTB was successfully encapsulated in the nanoemulsion formulation and this was confirmed by the analysis of EE.

The prepared formulation was subjected to further characterization of droplet size and PDI as shown in Table 1. The DNE was successfully prepared with a small droplet size in an acceptable nanometer range. A PDI of 0.26 indicated that the DNE formulation was monodispersed in the system, with a narrow size distribution. The nanosize character of the DNE formulation was confirmed by TEM images.

Measurement of morphology

The surface morphology of the DNE was studied by TEM. The photographs in Figure 1 reveal that all particles were slightly spherical, with a smooth surface.

Thermal properties analysis

DSC was used to investigate the thermal behavior of pure DTB in the nanoemulsion formulation, as shown in Figure 2. DTB showed an endothermic peak at 276.74°C, with onset at 272.79°C and end-set at 280.95°C, corresponding to the melting point of DTB. The DTB - nanoemulsion formulation showed an endothermic peak at 161.04°C with onset at 111.49°C and end-set at 182.46°C. The plain nanoemulsion formulation showed an endothermic peak at 161.92°C with onset at 124.83°C and end-set at 182.91°C.

Aerodynamic characterization

The aerodynamic behavior of the DNE formulation was measured at a flow rate of 15 L/min using the cascade impactor

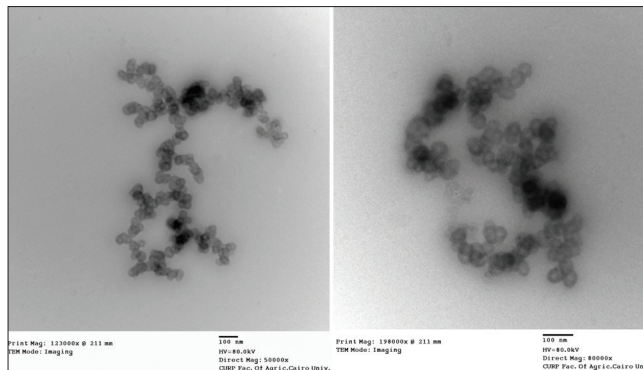


Figure 1: Transmission electron microscopy micrographs of Dasatinib-nanoemulsion

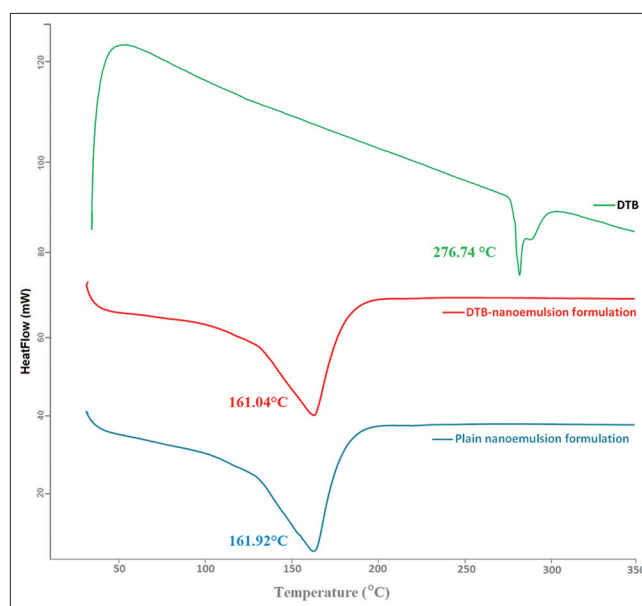


Figure 2: Thermal analysis of Dasatinib- nanoemulsion formulation

as shown in Table 2. The results in Table 2 show that the DNE formulation was delivered to the lungs and was considered to be respirable because the mean delivered dose of DTB was 8.558 ± 0.93 µg or $69.362 \pm 1.23\%$ of the TED, with good FPD and FPF. The result of MMAD showed an increase in the flow property of the DNE formulation which resulted in much better lung deposition, as shown in Figure 3.

In vitro cytotoxicity of DNE

Figure 4 shows the cell viability and cytotoxicity of the DNE formulation and DTB using A549 and Calu-3 lung cancer cells. The DNE formulation and free DTB suspension had an IC_{50}

value of 0.0431 $\mu\text{g/mL}$ and 0.166 $\mu\text{g/mL}$, respectively, on A549 lung cancer cells and had an IC_{50} value of 0.0443 $\mu\text{g/mL}$ and 0.0092 $\mu\text{g/mL}$, respectively, on Calu-3 lung cancer cells. The results in Figure 4 show that the anticancer activity of DNE formulation against A549 lung cancer cells was statistically (Student T-test, $P < 0.05$) greater than that of free DTB suspension.

Table 2: Aerodynamic behavior of DTB-nanoemulsion formulation

Formulation code	TED (μg)	FPD (μg)	FPF (%)	MMAD (μm)
DTB-nanoemulsion	12.338 \pm 1.35	3.819 \pm 0.47	44.631 \pm 5.12	4.202 \pm 0.59

TED: Total emitted dose, FPD: Fine-particle dose, FPF: Fine-particle fraction, MMAD: The mass median aerodynamic diameter

Cell cycle assay

Figure 5 shows the effect of the DNE formulation on cell cycle phases (G0/G1, S-phase, and G2/M-phase) of A549 lung cancer cells after 24 h and 48 h. The results of Figure 5 show that the mechanism of anticancer activity of DNE formulation against A549 lung cancer cells was through disruption of G2/M-phase cell replication. The G0/G1 cell population was significantly ($P < 0.05$) decreased from 62.51 \pm 1.77% for the control to 50.54 \pm 3.07% when treated with the DNE formulation after 24 h, while it was insignificantly ($P > 0.05$) increased from 53.17 \pm 1.16% for the control to 53.27 \pm 1.49% when treated with DNE formulation after 48 h. The S-phase cell population was significantly ($P < 0.05$) increased from 13.38 \pm 0.73% for the control to 20.49 \pm 1.54% when treated with DNE

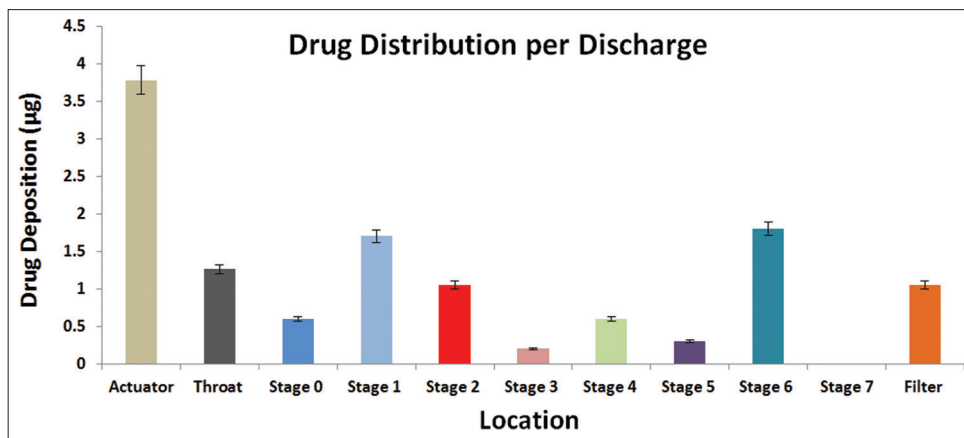


Figure 3: *In vitro* drug deposition of the Dasatinib-nanoemulsion formulation by the Cascade impactor

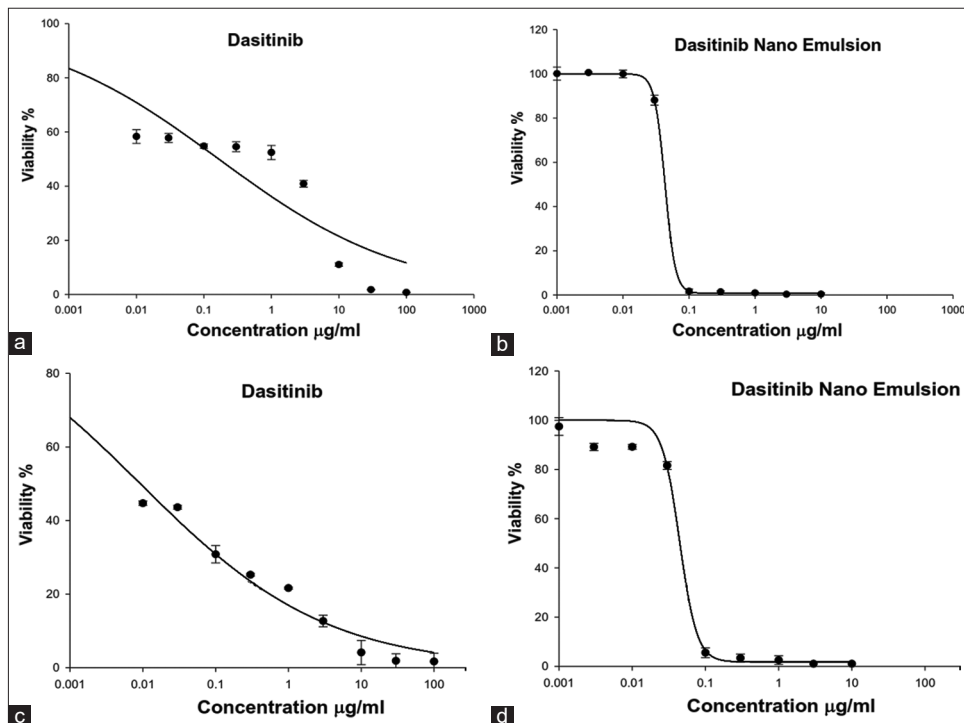


Figure 4: *In vitro* cytotoxicity of the Dasatinib (DTB)-nanoemulsion formulation and DTB against A549 (a and b) and Calu-3 (c and d) lung cancer cells

formulation after 24 h, while it was significantly ($P < 0.05$) decreased from $20.93 \pm 1.47\%$ for the control to $15.11 \pm 1.50\%$ when treated with DNE formulation after 48 h. The G2/M-phase cell population was significantly ($P < 0.05$) increased from $23.71 \pm 1.61\%$ for the control to $31.60 \pm 2.05\%$ when treated with DNE formulation after 24 h and was significantly ($P < 0.05$) increased from $23.41 \pm 1.92\%$ for the control to $31.34 \pm 2.21\%$ when treated with DNE formulation after 48 h.

Figure 6 shows the effect of the DNE formulation on cell cycle phases (G0/G1, S-phase, and G2/M-phase) of Calu-3 lung cancer cells after 24 h and 48 h. The results of Figure 6 show that the DNE formulation had anti-proliferative activity against Calu-3 lung cancer cells through disruption of the G0/G1-phase cell population. The G0/G1 cell population was significantly ($P < 0.05$) increased from $46.30 \pm 1.76\%$ for the control to $54.49 \pm 1.55\%$ when treated with DNE formulation after 24 h and was significantly ($P < 0.05$) increased from $54.91 \pm 2.85\%$ for the control to $60.72 \pm 2.60\%$ when treated with DNE formulation after 48 h. The S-phase cell population was insignificantly ($P > 0.05$) increased from $9.80 \pm 0.86\%$ for the control to $11.82 \pm 0.98\%$ when treated with DNE formulation after 24 h and was insignificantly ($P > 0.05$) increased from $10.44 \pm 1.08\%$ for the control to $10.71 \pm 0.69\%$ when treated with DNE formulation after 48 h. The G2/M-phase cell population was insignificantly ($P > 0.05$) increased from $30.17 \pm 1.54\%$ for the control to $31.38 \pm 1.48\%$ when treated with DNE formulation after 24 h and was significantly ($P < 0.05$)

increased from $33.71 \pm 2.21\%$ for the control to $38.39 \pm 1.48\%$ when treated with DNE formulation after 48 h.

Apoptosis assay

The effect of the DNE formulation on programmed cell death and apoptosis of A549 cancer cells after 24 h and 48 h was examined using a flow cytometry assay. Compared to the control cells, the DNE formulation showed a statistically significant ($P < 0.05$) decrease in the survival rate of A549 by 5.34% and 21.80% after 24 h and 48 h treatment, respectively. The results of Figure 7 show that the DNE formulation induced apoptosis against A549 lung cancer cells through the initiation of early and late apoptosis phases. Compared to the control cells, the DNE formulation showed insignificant ($P > 0.05$) induction in the early apoptosis phase of A549 after 24 h treatment by 0.35 folds while showed significant ($P < 0.05$) induction in the early apoptosis phase of A549 after 48 h treatment. Compared to the control cells, the DNE formulation showed significant ($P < 0.05$) induction in the late apoptosis phase of A549 after 24 h treatment while showed significant ($P < 0.05$) induction in the late apoptosis phase of A549 after 48 h treatment. The effect of the DNE formulation on programmed cell death and apoptosis of Calu-3 cancer cells after 24 h and 48 h was examined as shown in Figure 8. Compared to the control cells, the DNE formulation showed a statistically significant ($P < 0.05$) decrease in the survival rate of Calu-3 by 29.03% and 51.37% after 24 h and 48 h treatment, respectively.

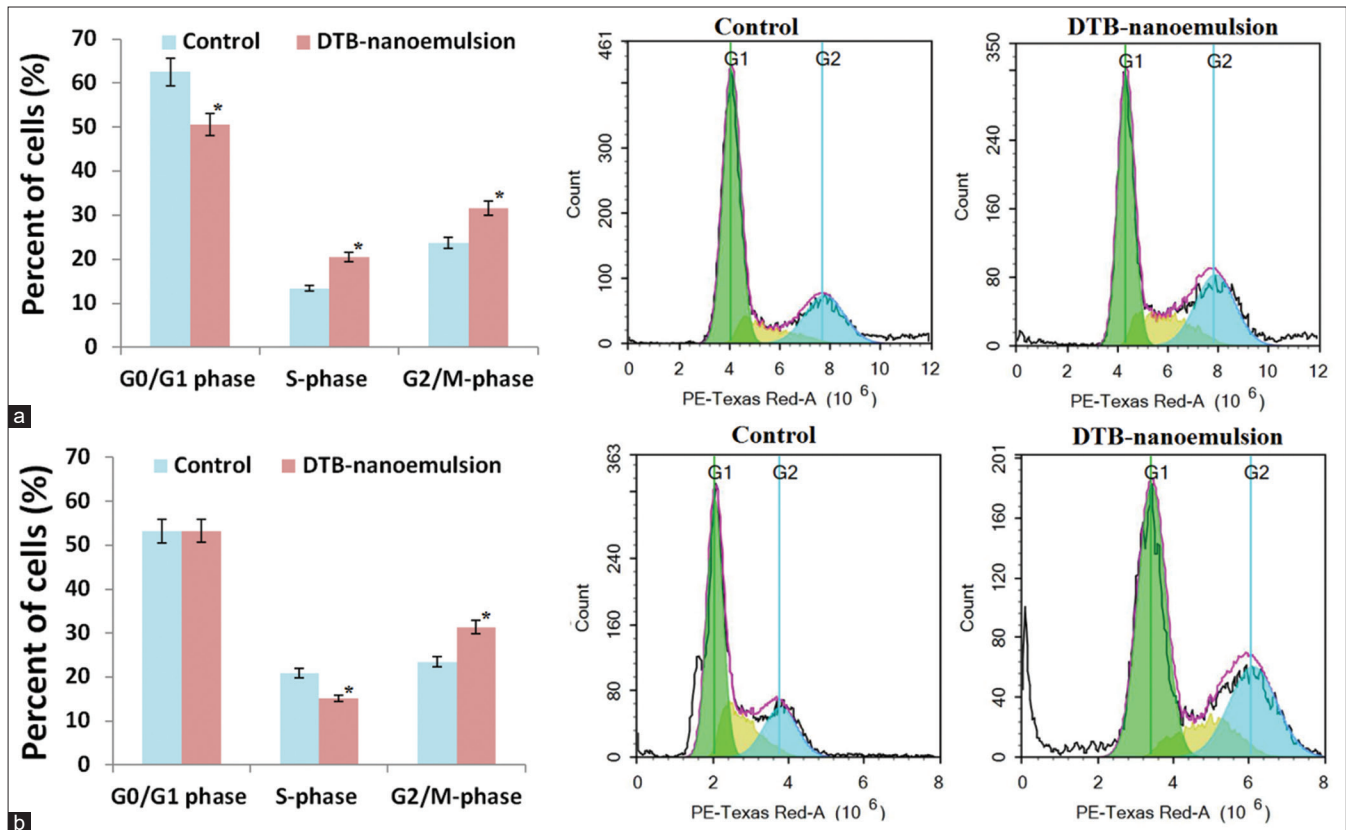


Figure 5: The effect of Dasatinib-nanoemulsion on cell cycle phases of A549 lung cancer cell lines; (a) 24 h and (b) 48 h

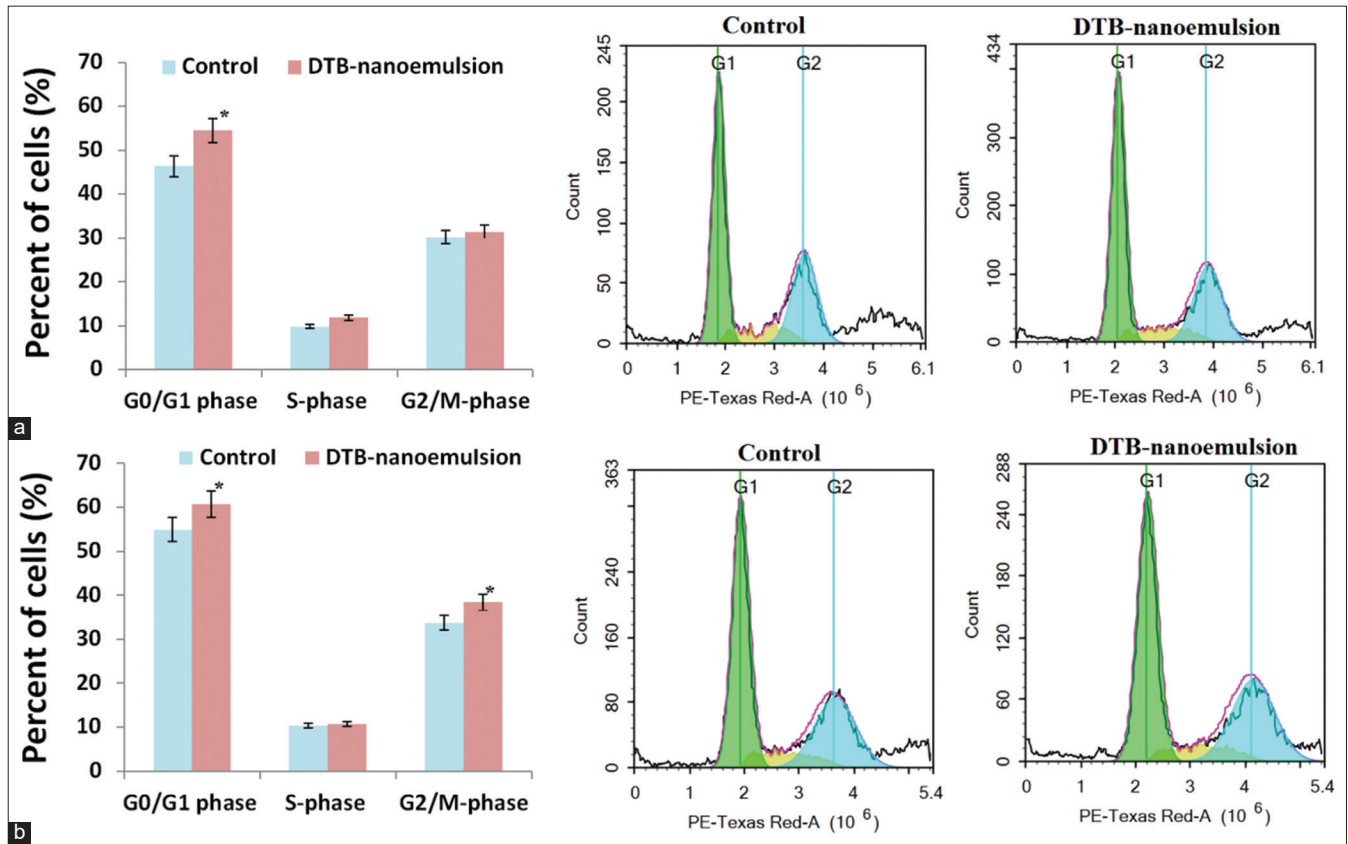


Figure 6: The effect of Dasatinib-nanoemulsion on cell cycle phases of Calu-3 lung cancer cell lines; (a) 24 h and (b) 48 h

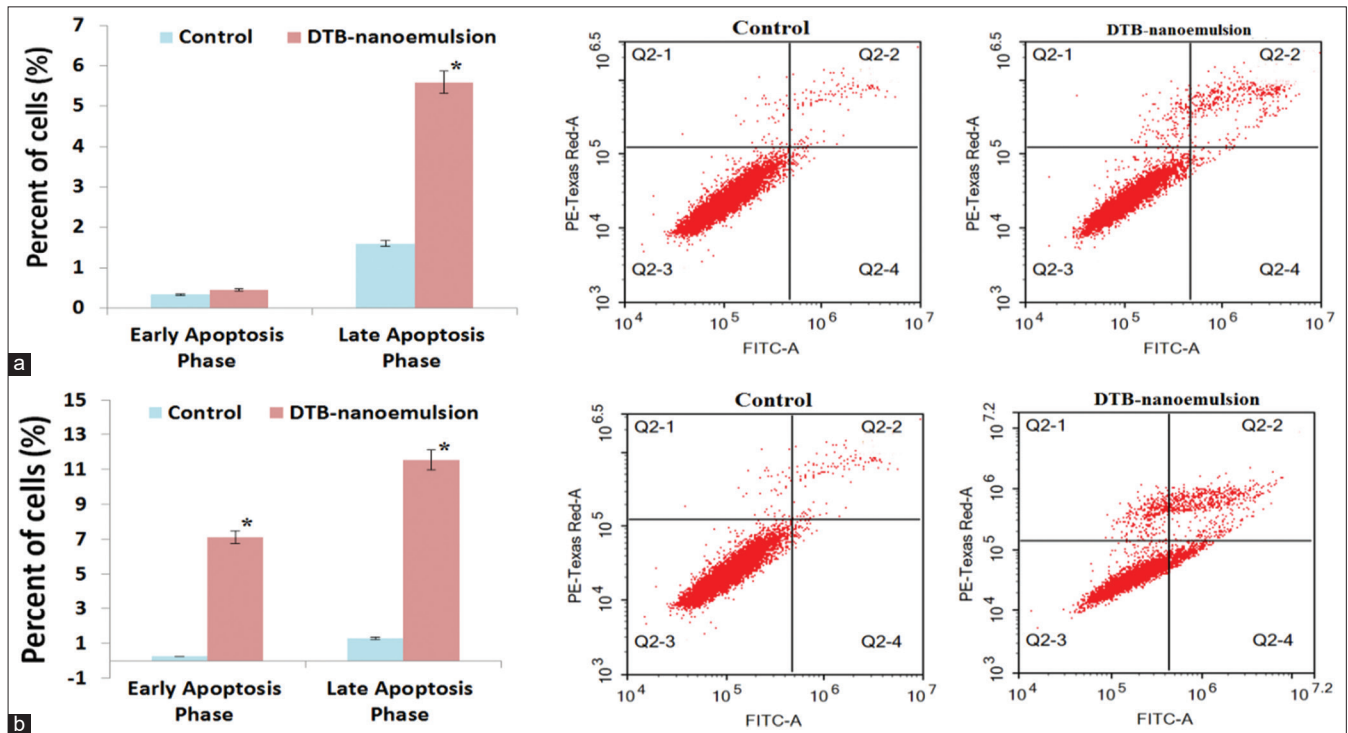


Figure 7: Programmed cell death and apoptosis of A549 cancer cells; (a) 24 h and (b) 48 h

The effect of the DNE formulation on programmed cell death and apoptosis of Calu-3 cancer cells after 24 h and 48 h was

examined as shown in Figure 8. Compared to the control cells, the DNE formulation showed a statistically significant

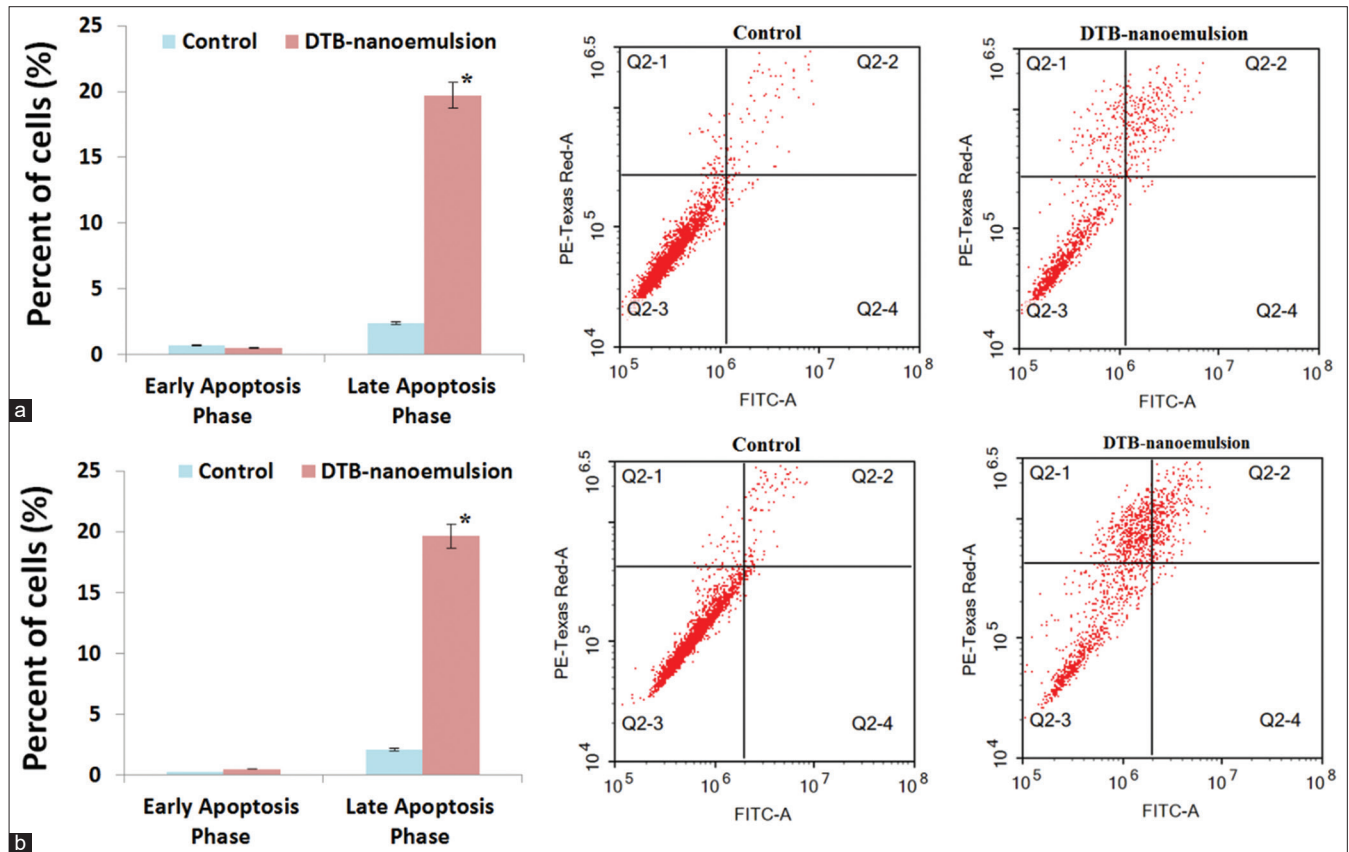


Figure 8: Programmed cell death and apoptosis of Calu-3 cancer cells; (a) 24 h and (b) 48 h

($P < 0.05$) decrease in the survival rate of Calu-3 by 29.03% and 51.37% after 24 h and 48 h treatment, respectively.

The results in Figure 8 show that the DNE formulation induced apoptosis against Calu-3 lung cancer cells through the initiation of late apoptosis phases.

Compared to the control cells, the DNE formulation showed a negative effect on the early apoptosis phase of Calu-3 after 24 h treatment while showing insignificant ($P > 0.05$) induction in the early apoptosis phase of Calu-3 after 48 h treatment. Compared to the control cells, the DNE formulation showed significant ($P < 0.05$) induction in the late apoptosis phase of Calu-3 after 24 h treatment, and again showed significant ($P < 0.05$) induction in the late apoptosis phase of Calu-3 after 48 h treatment.

Discussion

To determine the composition of the nanoemulsion (type of oil phase, type of non-ionic surfactants, and ratio of oil to non-ionic surfactants), a review of the literature and pre-formulation studies was conducted.^[37-39] Oleic acid was used as the oil phase due to its high solvency.^[37,39] Because oleic acid is a powerful penetration enhancer, it was utilized to serve a dual purpose as a delivery system component and to assess the solubility of DTB in oleic acid.^[40] The solubility of DTB in oleic acid results was good and similar results were

obtained by Sravanthi *et al.* who investigated the effect of oleic acid nanoemulsion as a delivery vehicle for nasal vaccination and found that the use of oleic acid as oil phase substantially increased penetration ability through the nasal mucosa and augmented the immune response.^[40] The surface-active agent had an extensive influence on the nanoemulsion.^[38,40]

It was used to stabilize the nanoemulsion by reducing interfacial tension and preventing the formation of flocculation and coalescence of dispersed phase droplets of such systems.^[38,40]

Kolliphor RH 40 was used as a nonionic solubilizer and emulsifying agent.^[35,36] To produce a nanoemulsion with small droplet size and narrow size distribution, a lower temperature was helpful. RH 40's hydrophilicity increased as the temperature dropped, which led to an impressive decrease in the oil–water interfacial tension and the ability to create a stable nanoemulsion with small droplet sizes.^[35,36] To create the nanoemulsion, a temperature of 20°C was selected based on RH 40, which showed a good connection at the oil–water interface. This is consistent with Christina *et al.*, who found that the use of Kolliphor RH 40 as a nonionic surfactant at room temperature enhanced the development and stability of a new nanoemulsion formulation.^[36]

Dipropylene glycol served as a cosurfactant by adsorbing at the oil–water interface and further lowering the interfacial

tension.^[41,42] Because the nanoemulsion's drug-loading capacity and droplet size were thoroughly taken into account, the formulation composed functioned successfully for spontaneous emulsification.

Physiochemical evaluation of DNE

Medication encapsulation and content efficiency were assessed, and the findings of the drug content demonstrated that employing the nanoemulsion formulation had successfully improved the aqueous solubility of DTB. The greater solubility of oleic acid and the critical function of amphiphilic surfactants (Span 60 and Tween 60) in lowering interfacial tension may provide insight into these findings. Similar results were obtained by Gupta who enhanced the efficacy, permeability, and bioavailability of aceclofenac for the treatment of arthritis using nanoemulsion.^[37] The DNE was successfully prepared with a small droplet size in an acceptable nanometer range. The DNE formulation was monodisperse in the system with narrow size distribution, according to the PDI. TEM pictures also verified the DNE formulation's nanoscale. After TEM was used to examine the DNE's surface morphology. All of the particles were found to have smooth surfaces and were slightly round.

The thermal properties of pure DTB were analyzed using DSC. It was noted that there was a shift in the melting point of DTB, indicating that DTB was molecularly dispersed in the nanoemulsion formulation. The complete fusion of DTB in the matrix was further proved by the thermograms of plain nanoemulsion components. In addition, when the DNE formulation's aerodynamic behavior was tested, the total emitted dosage, FPD, and FPF were all within a good range. Because droplet size affects both the deposition site and the amount of inhaled drug that is deposited in the respiratory system, MMAD was measured.^[21] The result of MMAD showed increased flow property in the DNE formulation, which resulted in much better lung deposition. Figure 3 also confirms that the deposition of DNE formulation after aerosolization on ACI stages was flowable because the distribution of the deposited dose of DTB was mainly in the alveoli (stage 6).

Bio- characterization of DNE

The *in vitro* cell viability and cytotoxicity of the DNE formulation and free DTB were studied using A549 and Calu-3 lung cancer cells. The findings indicated that the DNE formulation exhibited anticancer activity against A549 lung cancer cells that was statistically significantly higher than the free DTB solution. This enhanced anticancer activity could be due to the solubilizing effect of nanoemulsion leading to enhanced DTB release and aqueous solubility, consequently improving the bioavailability of DTB. The synergistic effect of oleic acid/non-ionic surfactants on DTB may account for its increased penetration. These observations suggested that the nanoemulsion formulation could be a workable DTB carrier and a useful tactic for treating lung cancer.

In addition, the antiproliferative effect of DNE can be influenced using cell cycle assessment in terms of G0/G1, S-phase, and G2/M-phase for cell cycle phase specificity^[21,43] as G0/G1-phase denotes non-proliferating cells. Compounds with antiproliferative effects are expected to increase this cell population significantly. S-phase denotes proliferating cells and particularly cells which are undergoing the DNA synthesis step of replication. Some compounds might induce S-phase arrest and increase this cell population significantly. G2/M-phase indicates the final phase of cell replication (mitosis). Compounds interfering with microtubular spindles (stabilize or destabilize) are expected to increase this cell population significantly. The effect of the DNE formulation on cell cycle phases G0/G1, S-phase, and G2/M-phase of A549 lung cancer cells after 24 h and 48 h was studied and found that the mechanism of the anticancer activity of the DNE formulation against A549 lung cancer cells was through disruption of G2/M-phase cell replication. These findings were consistent with a prior study that found that DTB nanoemulsion-exposed A549 cancer cells were arrested in the G2/M phase.^[7]

In addition, the effect of the DNE formulation on cell cycle phases G0/G1, S-phase, and G2/M-phase of Calu-3 lung cancer cells after 24 h and 48 h was studied. It was found that the DNE formulation had anti-proliferative activity against Calu-3 lung cancer cells through disruption of the G0/G1-phase cell population. Based on these findings, we conclude that the DNE formulation was able to significantly arrest the cell cycle in A549 and Calu-3 lung cancer cells. This suggests that this nanoemulsion may be a viable vehicle for DTB for use as a substitute for the effective treatment of small-cell lung cancer.

Furthermore, the apoptosis assay of the DNE formulation was studied. As a potential cancer treatment intention, programmed cell death or apoptosis is deemed significant.^[44,45] The early apoptosis phase Q4 denotes cells that have just initiated the apoptosis programmed cell death process with their cell membrane still intact. The late apoptosis phase Q2 denotes cells that have initiated the apoptosis-programmed cell death process with their cell membrane perforated. Normal intact cells are represented by the cell population in the Q3 segment.

The effect of the DNE formulation on programmed cell death and apoptosis of A549 cancer cells after 24 h and 48 h was examined using a flow cytometry assay. Through the start of the early and late apoptosis phases, the DNE formulation caused apoptosis in A549 lung cancer cells. The DNE formulation demonstrated a 0.35-fold increase in the early apoptotic phase of A549 after 24 h of treatment, and a 27.82-fold increase in the same phase of A549 after 48 h of treatment, as compared to the control cells. In comparison to the control cells, the late apoptotic phase of A549 demonstrated a 2.50-fold increase following a 24-h treatment with the DNE formulation and an 8.03-fold increase following a 48-h therapy. This result was consistent with the study conducted by Johnson *et al.*^[46]

The effect of the DNE formulation on apoptosis and programmed cell death in Calu-3 cancer cells was also investigated after 24 and 48 h. After both treatment periods with the DNE formulation, Calu-3 lung cancer had a lower survival rate compared to the control cells. This suggests that the formulation's mechanism of inducing apoptosis against Calu-3 lung cancer cells involved the onset of late apoptosis phases.

The DNE formulation, in comparison to the control cells, demonstrated an inverse relationship with the early apoptotic phase of Calu-3 following a 24-h treatment, and a 0.8-fold induction of this phase following a 48-h treatment. The DNE formulation increased Calu-3's late apoptotic phase induction by 7.29 times after 24 h of treatment and by 8.28 times after 48 h of treatment, as compared to the control cells.

According to these findings, exposure to the DNE formulation induced a significant amount of apoptosis in A549 and Calu-3 lung cancer cells. This suggests that nanoemulsion could be a viable vehicle for DTB and be utilized as an alternative for the successful treatment of small-cell lung cancer.

Conclusion

The current study aimed to develop DTB nanoemulsion as an inhalation for improving DTB's delivery and efficacy as a potential lung cancer treatment. It was shown that the DNE formulation improved the aqueous solubility of DTB and produced nanoparticles with an entrapment efficiency of 96.74% and small, narrow droplet size distribution. Compared with free DTB, the DNE formulation increased the flow property of DTB and delivered it to the lungs with good FPD, FPF, and MMAD. The anticancer activity of the DNE formulation against A549 and Calu-3 lung cancer cells was significantly higher (p-value <0.05) than that of DTB. These results made it clear that the nanoemulsion formulation might be a viable DTB carrier that could be used as a strategy for successful lung cancer treatment.

The limitations of the work are the need for evaluation of the toxicity, efficacy, and pharmacokinetics of DNE formulations using animal models. Therefore, future research endeavors will focus on assessing the toxicity, efficacy, and pharmacokinetics of such formulations through animal model evaluation. This research could offer valuable insights into the safety, effectiveness, and distribution of these formulations in living organisms, paving the way for potential therapeutic applications. By systematically evaluating these parameters, researchers can better understand the potential risks and benefits associated with DNE formulations, thereby informing future clinical trials and regulatory decisions. In addition, such research may also contribute to advancements in nanoemulsion technology and drug delivery systems, offering new opportunities for targeted and efficient drug delivery.

Ethics Approval and Consent to Participate

In preparing this article, the authors conducted no experiments on animals and humans.

Availability of Data and Materials

Datasets used during this investigation can be obtained from the corresponding author.

Competing Interests

The authors report no conflicts of interest, either financial or otherwise.

Funding

This study has not received any external funding.

Authors' Contributions

The author confirms sole responsibility for the manuscript preparation, study conception, and data/results collection and analysis.

References

- Ahmad S, Khan MY, Rafi Z, Khan H, Siddiqui Z, Rehman S, *et al.*, editors. Oxidation, glycation and glycoxidation-the vicious cycle and lung cancer. In: *Seminars in Cancer Biology*. Elsevier; 2018.
- Lundin A, Driscoll B. Lung cancer stem cells: Progress and prospects. *Cancer Lett* 2013;338:89-93.
- Schabath MB, Cote ML. Cancer progress and priorities: Lung cancer. *Cancer Epidemiol Biomarkers Prev* 2019;28:1563-79.
- Li S, Xu S, Liang X, Xue Y, Mei J, Ma Y, *et al.* Nanotechnology: Breaking the current treatment limits of lung cancer. *Adv Healthc Mater* 2021;10:2100078.
- Gelatti AC, Drilon A, Santini FC. Optimizing the sequencing of tyrosine kinase inhibitors (TKIs) in epidermal growth factor receptor (EGFR) mutation-positive non-small cell lung cancer (NSCLC). *Lung Cancer* 2019;137:113-22.
- Song L, Morris M, Bagui T, Lee FY, Jove R, Haura EB. Dasatinib (BMS-354825) selectively induces apoptosis in lung cancer cells dependent on epidermal growth factor receptor signaling for survival. *Cancer Res* 2006;66:5542-8.
- Zhang M, Tian J, Wang R, Song M, Zhao R, Chen H, *et al.* Dasatinib inhibits lung cancer cell growth and patient derived tumor growth in mice by targeting LIMK1. *Front Cell Dev Biol* 2020;8:556532.
- Garmendia I, Pajares MJ, Hermida-Prado F, Ajona D, Bértolo C, Sainz C, *et al.* YES1 drives lung cancer growth and progression and predicts sensitivity to dasatinib. *Am J Respir Crit Care Med* 2019;200:888-99.
- Zhang J, Chen Y, He Q. Distinct characteristics of dasatinib-induced pyroptosis in gasdermin E-expressing human lung cancer A549 cells and neuroblastoma SH-SY5Y cells. *Oncol Lett* 2020;20:145-54.
- Niza E, Nieto-Jiménez C, Noblejas-López MM, Bravo I, Castro-Osma JA, de la Cruz-Martínez F, *et al.* Poly (cyclohexene phthalate)

- nanoparticles for controlled dasatinib delivery in breast cancer therapy. *Nanomaterials* (Basel) 2019;9:1208.
11. Hořínková J, Šíma M, Slanař O. Pharmacokinetics of dasatinib. *Prague Med Rep* 2019;120:52-63.
 12. Aboubakr EM, Mohammed HA, Hassan AS, Mohamed HB, El Dosoky MI, Ahmad AM. Glutathione-loaded non-ionic surfactant niosomes: A new approach to improve oral bioavailability and hepatoprotective efficacy of glutathione. *Nanotechnol Rev* 2021;11:117-37.
 13. Mohamed MS, El-Shenawy AA, Mahmoud EA, Amin MA, Mohammed HA, Shaldam MA, *et al.* Metolazone co-crystals-loaded oral fast dissolving films: Design, optimization, and *in vivo* evaluation. *J Drug Deliv Sci Technol* 2023;90:105167.
 14. Mohan A, Sangeetha G. Formulation and evaluation of immediate release film coated tablets of an anticancer drug (dasatinib). *Res J Pharm Technol* 2019;12:729-34.
 15. Parvataneni DM, Devraj R, Mangamoori LN. Micelles entrapped microparticles technology: A novel approach to resolve dissolution and bioavailability problems of poorly water soluble drugs. *J Microencapsul* 2020;37:254-69.
 16. Begum M, Gudipati P. Formulation and evaluation of dasatinib loaded solid lipid nanoparticles. *Int J Pharm Pharm Sci* 2018;10:14-20.
 17. McClements DJ, Rao J. Food-grade nanoemulsions: Formulation, fabrication, properties, performance, biological fate, and potential toxicity. *Crit Rev Food Sci Nutr* 2011;51:285-330.
 18. Rai VK, Mishra N, Yadav KS, Yadav NP. Nanoemulsion as pharmaceutical carrier for dermal and transdermal drug delivery: Formulation development, stability issues, basic considerations and applications. *J Control Release* 2018;270:203-25.
 19. Gamal A, Saeed H, Sayed OM, Kharshoum RM, Salem HF. Proniosomal microcarriers: Impact of constituents on the physicochemical properties of proniosomes as a new approach to enhance inhalation efficiency of dry powder inhalers. *AAPS PharmSciTech* 2020;21:1-12.
 20. Peng T, Lin S, Niu B, Wang X, Huang Y, Zhang X, *et al.* Influence of physical properties of carrier on the performance of dry powder inhalers. *Acta Pharm Sin B* 2016;6:308-18.
 21. Tulbah AS, Gamal A. Design and characterization of atorvastatin dry powder formulation as a potential lung cancer treatment. *Saudi Pharm J* 2021;29:1449-57.
 22. Khairnar SV, Jain DD, Tambe SM, Chavan YR, Amin PD. Nebulizer systems: A new frontier for therapeutics and targeted delivery. *Ther Deliv* 2022;13:31-49.
 23. Newman S. Metered dose pressurized aerosols and the ozone layer. *Eur Respir J* 1990;3:495-7.
 24. Bouchemal K, Briancón S, Perrier E, Fessi H. Nano-emulsion formulation using spontaneous emulsification: Solvent, oil and surfactant optimisation. *Int J Pharm* 2004;280:241-51.
 25. Alarjah MA, Shahin MH, Al-Azzah F, Alarjah AA, Omran ZH. Concomitant analysis of dasatinib and curcuminoids in a pluronic-based nanoparticle formulation using a novel HPLC method. *Chromatographia* 2020;83:1355-70.
 26. Bhattacharyya S, Reddy P. Effect of surfactant on azithromycin dihydrate loaded stearic acid solid lipid nanoparticles. *Turk J Pharm Sci* 2019;16:425.
 27. Dixit M, Kini A, Kulkarni P. Preparation and characterization of microparticles of piroxicam by spray drying and spray chilling methods. *Res Pharm Sci* 2010;5:89.
 28. Salem H, Abdelrahim M, Eid KA, Sharaf M. Nanosized rods agglomerates as a new approach for formulation of a dry powder inhaler. *Int J Nanomed* 2011;6:311.
 29. Pharmacopeia U.S. USP 39-NF34. The United States Pharmacopeial 2016
 30. Anderson, S. The British Pharmacopoeia, 1864 to 2014: Medicines, international standards and the state by anthony C. Cartwright. *Bull Hist Med* 2016;90:340-342.
 31. Marin L, Traini D, Bebawy M, Colombo P, Buttini F, Hagni M, *et al.* Multiple dosing of simvastatin inhibits airway mucus production of epithelial cells: Implications in the treatment of chronic obstructive airway pathologies. *Eur J Pharm Biopharm* 2013;84:566-72.
 32. Allam RM, Al-Abd AM, Khedr A, Sharaf OA, Nofal SM, Khalifa AE, *et al.* Fingolimod interrupts the cross talk between estrogen metabolism and sphingolipid metabolism within prostate cancer cells. *Toxicol Lett* 2018;291:77-85.
 33. Tulbah AS, Pisano E, Landh E, Scalia S, Young PM, Traini D, *et al.* Simvastatin nanoparticles reduce inflammation in LPS-stimulated alveolar macrophages. *J Pharm Sci* 2019;108:3890-7.
 34. Fekry MI, Ezzat SM, Salama MM, Alshehri OY, Al-Abd AM. Bioactive glycoalkaloides isolated from *Solanum melongena* fruit peels with potential anticancer properties against hepatocellular carcinoma cells. *Sci Rep* 2019;9:1746.
 35. Bunchongprasert K, Shao J. Cytotoxicity and permeability enhancement of Capmul® MCM in nanoemulsion formulation. *Int J Pharm* 2019;561:289-95.
 36. Chrastina A, Welsh J, Borgström P, Baron VT. Propylene glycol caprylate-based nanoemulsion formulation of plumbagin: Development and characterization of anticancer activity. *Biomed Res Int* 2022;2022:3549061.
 37. Gupta SK. Formulation and evaluation of nanoemulsion based nanoemulgel of aceclofenac. *J Pharm Sci Res* 2020;12:524-32.
 38. Mishchenko E, Timofeeva E, Artamonov A, Portnaya I, Koroleva MY. Nanoemulsions and nanocapsules with oleic acid. *Colloid J* 2022;84:64-70.
 39. Permyakova I, Vol'khin V, Kazakov D, Kaczmarek K, Kudryashova O, Sukhoplechova E. Phase equilibria in triacylglycerols-ethanol-oleic acid-ethyl oleate quasi-quaternary system. *Eur Chem Technol J* 2014;16:257-64.
 40. Sravanthi V, Pallavi MP, Bonam SR, Sathyabama S, Kumar HM. Oleic acid nanoemulsion for nasal vaccination: Impact on adjuvanticity based immune response. *J Drug Deliv Sci Technol* 2015;28:56-63.
 41. Jadhav C, Shinde S, Kate V, Payghan S. Investigating application of non-aqueous microemulsion for drug delivery. *Asian J Biomed Pharm Sci* 2014;4:1-9.
 42. Chen C, Shen H, Harwell JH, Shiao BJ. Characterizing oil mixture and surfactant mixture via hydrophilic-lipophilic deviation (HLD) principle: An insight in consumer products development. *Colloids Surf A Physicochem Eng Aspects* 2022;634:127599.
 43. Kuh HJ, Nakagawa S, Usuda J, Yamaoka K, Saijo N, Nishio K. A computational model for quantitative analysis of cell cycle arrest and its contribution to overall growth inhibition by anticancer agents. *Jpn J Cancer Res* 2000;91:1303-13.
 44. Abdelfadil E, Cheng YH, Bau DT, Ting WJ, Chen LM, Hsu HH, *et al.* Thymoquinone induces apoptosis in oral cancer cells through p38 β inhibition. *Am J Chin Med* 2013;41:683-96.
 45. Hwang JM, Ting WJ, Wu HC, Chen YJ, Tsai FJ, Chen PY, *et al.* KHC-4 anti-cancer effects on human PC3 prostate cancer cell line. *Am J Chin Med* 2012;40:1063-71.
 46. Johnson FM, Saigal B, Talpaz M, Donato NJ. Dasatinib (BMS-354825) tyrosine kinase inhibitor suppresses invasion and induces cell cycle arrest and apoptosis of head and neck squamous cell carcinoma and non-small cell lung cancer cells. *Clin Cancer Res* 2005;11:6924-32.